IMAGING GAS COUNTERS FOR X- AND GAMMA RAY ASTRONOMY

BRIAN D. RAMSEY
NASA/MSFC, Huntsville, Alabama 35812, USA

Abstract. Gas-filled detectors, such as proportional counters, have long been used in x-ray astronomy. They are robust, relatively easy to fabricate, and can provide large collecting areas with reasonable spatial and energy resolution. Despite coming of age in the 50's and 60's, their versatility is such that they are still planned for future missions. A vigorous development program, led mostly by the high energy physics community, has ensured continued improvements in proportional counter technology. These include multistep counters, microstrip technologies and optical avalanche chambers. High fill-gas pressures and the use of suitable converters permit operation up to 100s of GeV. The current status of imaging gas-filled detectors will be reviewed, concentrating on the lower energy region (< 100 keV) but also briefly covering higher energy applications up to the GeV region. This review is not intended to be exhaustive and draws heavily on work currently in progress at MSFC.

Key words: X-Rays – Imaging – Gas-filled Detectors – Proportional Counters

1. Introduction

Imaging proportional counters have been used extensively for x-ray / gamma ray astronomy from small-area, low-energy devices at the focus of x-ray telescopes (e.g. ROSAT [1]) to larger stand-alone devices at higher energies such as the TTM experiment on MIR [2]. In addition, they are planned for future missions such as Spectrum-X [3] and INTEGRAL [4]. The reason for their popularity is obvious - they are relatively easy to fabricate in the large areas necessary for non-focusing imaging, they are robust and reliable, and they offer reasonable performance in terms of spatial resolution, energy resolution, timing and background rejection. Fig. 1a shows the efficiency of a xenon-filled gas detector as a function of energy. Below 100 keV, large efficiencies can be obtained with modest fill gas pressures (< 5 atm) in large (1000(s) cm^2) single-volume chambers. For higher energies, where the fill-gas pressure initially rises rapidly, standard vessels quickly become very bulky, window arrangements become difficult, and so modular approaches arraying large numbers of small, thin-walled tubular pressure vessels are typically proposed. Nevertheless, because of the high compressibility of xenon and rising pair-production cross-section, even MeV-GeV photons can be efficiently absorbed at achievable fill-gas pressures.

Fig. 1b shows the photoelectron-range-limited spatial resolution, achievable at various fill gas pressures. Since most readout schemes give a center of gravity of the primary charge cloud, this typically represents the resolution achievable on axis, especially below 100 keV where large-area imaging devices are used [5]. Typical readout schemes, particularly those utilizing

Experimental Astronomy **6**: 119–127, 1995.

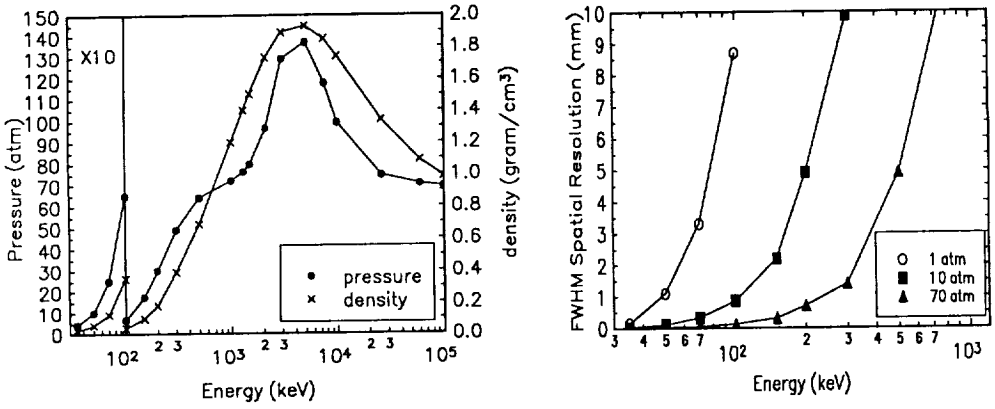

Fig. 1. a and b : (a) The pressure (left axis) and density (right axis) needed to give 50% detection efficiency in 10 cm of xenon; the data below 100 keV are expanded (y scale x 10) for clarity. (b) Photoelectron range limited spatial resolution for various fill-gas pressures. Line is intended to guide eye only.

large numbers of preamplifiers on individual, or groups of, cathode wires, have very low noise and can reconstruct the center of gravity of the charge cloud with high precision. Other schemes, such as delay line readout [3], offer similar performance. Above 100 keV, at intermediate energies where multiwire imaging chambers are not typically employed, spatial resolution is limited by other factors, such as the readout scheme or detector size for modular arrays. For very high energies (MeV-GeV), the highly extended electron tracks can be reconstructed to derive sub-mm spatial resolution once more.

2. General techniques for improving performance of proportional counters

2.1 Fluorescence gating

Standard background-rejection uses anticoincidence and pulse-shape discrimination and routinely achieves >95% rejection below about 10 keV; these schemes are, however, less efficient at higher energies. To combat this, xenon-filled detectors can utilize fluorescence gating, which exploits the fact that most photon interactions ($\simeq$75%) above 35 keV (and below 300 keV) result in fluorescence, the reabsorption of which results in a pair of events that are a characteristic signature of true x-ray interactions. Imaging gas detectors can be designed to resolve these pairs of events with high efficiency.

For cases where the non-aperture flux dominates, fluorescence gating can provide a large background reduction. Measurements of the ratio of pair

events to single events, give 1:2 for low-energy photons (<100 keV) but 1:50 for high energy photons (662 keV) and charged particles [6]. Fluorescence gating also provides a true energy measure of photoelectric interactions (no escaping photons) and improves energy resolution (by a factor of two at 40 keV) because the precise energy of one of of the two events is known. Furthermore, the ability to resolve the two events (rather than using an energy -weighted mean position), improves spatial resolution. There is, however, a small energy band (near 60 keV) where it is difficult to exploit these advantages.

2.2 Penning gas mixtures

In xenon gas, the average energy to form an electron-ion pair (21 eV) is almost twice the ionization potential (12 eV). Thus about half of the available energy is lost from the signal. Much of this "lost" energy appears in long-lived metastable states. The Penning effect uses a quench gas, with ionization potential matched to the principal metastable energy of the working gas, that becomes collisionally ionized while resonantly de-exciting the working gas. The increased number of electrons enhances energy resolution and allows a lower operating voltage. A comprehensive study of quench additives for xenon [7] found the strongest Penning effect with trimethylamine $(CH_3)_3N$, and a weaker effect with isobutylene (i-C_4H_8).

2.3 Effect of anode diameter/field configuration

The energy resolution of a gas counter is given by $2.36\ (((F+f)W)/E)^{0.5}$ where E is the energy of the x-ray, W is the mean ionization energy for the fill gas (21 eV for xenon), F is the Fano factor (0.16 for xenon) and f is the variance of gas amplification for 1 electron (typically 0.6-0.8). The theoretical work of Alkhazov [8] showed that f depends on the quantity $X=\alpha V_i/E$ where α is the Townsend coefficient, V_i is the gas ionization potential and E is the electric field strength. Higher X implies greater ionization efficiency and lower variance in the distribution of electrons in the avalanche. In general X increases with electric field, as α is a strong function of E, and thus fine anodes and close anode-to-cathode spacings are most desirable. Unfortunately, because of disruptive electrostatic forces, this is difficult to achieve in multiwire chambers. However, the microstrip proportional counter, detailed below, offers the possibility of proportional counters with extremely fine anodes and high packing density.

3. Some new instruments

3.1 Low energy region (<100 keV)

3.1.1 Microstrip gas detectors

The microstrip detector replaces the usual discrete cathode and anode wire planes with conducting strips on an insulating or partially insulating substrate. Originated by Oed [9] to replace the conventional wire imaging proportional counter, it offers numerous advantages; ease of construction, more uniform response, reduction in operating voltage for a given gain, reduced charge saturation at high gain, ability to operate with little or no quench gas, better energy resolution, enhanced spatial resolution, and higher efficiency for the detection of fluorescence pairs [10]. At least two groups have been actively developing microstrips for x-ray astronomy - the Danish Space Research Institute [11], and MSFC [12]. In addition, the microstrip is being considered for the readout in a proposed X-Ray Monitor (XRM) for INTEGRAL [4].

The microlithographic techniques used for production of microstrips permit exceptional spatial accuracy (1 μm) and uniformity, as well as extremely fine (1 μm) electrodes. These features improve gain uniformity - we have measured (1-σ) gain variations of only 1% over the area (25 cm^2) of test detectors fabricated using electron-beam technology. For comparison, in a conventional wire chamber, mechanical innacuracies and electrostatic forces typically give gain variations of 20% or more.

Microstrip technology also permits an electrode pitch much finer than the 1-to-2-mm minimum in a wire chamber and anode widths significantly less than the 15-to-25 μm practical minimum for uniform wires. The former distributes the charge signal over many anodes; the latter produces intense electric fields which effect very fast ion collection times. Together, these result in reduced charge saturation at high gain. Other benefits of fine-scale geometry include substantially reduced operating voltages and the ability to operate efficiently without a quench gas. The latter arises from the high electric fields, which channel a larger portion of the avalanche energy into ionization rather than excitation. Using little or no quench gas minimizes radiation-aging effects and improves reliability.

The high electric field also enhances energy resolution (section 2.3). Measurements as a function of decreasing wire diameter (down to a practical minimum of 12.5 μm) or width (microstrip) show gradually improving resolution, verifying the predictions of Alkhazov. To date, the best resolution achieved in xenon is just over 6% at 22 keV with 8 μm anodes and 200 μm anode/cathode separation [10]. Microstrips with anode widths down to 1μm are currently being tested. The ability to configure the electrodes at essentially any pitch also is important for imaging. Physics limited resolution (Fig 1a) is easily achievable at low energies due to the large gains available.

Practical problems in fabricating large-area microstrips have recently dissappeared and now several companies have equipment capable of writing masters up to $(40\ cm)^2$. A large area $(30\ cm)^2$ microstrip has recently been developed for the MSFC balloon program using one of these large format devices [12].

Finally, an important issue for space applications is the stability and possible lifetime of microstrips. These are related to the choice of substrate which must be chosen so as to have enough surface conductivity to prevent charge build-up and yet keep leakage current low to minimize noise. To date most work has concentrated on ionic conduction glasses (10^6 - 10^8 ohm-cm at 250°C) which, after an initial settling time of order 1 hour after bias is applied, operate stably to very high rates, but do exhibit small gain variations with time (10% over a few weeks). Recently a new type of glass has become available having electronic rather than ionic conduction. The ohmic behavior of this glass results in predictable performance and offers the prospect of stable operation over long periods. Initial results (at CERN and elsewhere) look very encouraging and the material is currently being evaluated at MSFC. The lifetime of the microstrip should not be a problem with the very low count rates in orbit, particularly if only very tiny quantities of quench gas are used. Reports of permanent damage are typically at very high fluences ($10^9/mm^2$) or at high count rates ($10^5/mm^2$ sec). In addition, we see no signs of damage either from proton irradiation of the substrate (10 Mrad) or from alpha irradiation of the operating microstrip ($10^8/cm^2$).

3.1.2 The optical avalanche chamber

While electron multiplication in high field regions results in increased ionization, multiplication in very low fields gives large amounts of excitation. Such low-field conditions are met in the parallel-plate proportional chamber, where the avalanche extends over several mm. The addition of photosensitive quench gases to such chambers, termed optical avalanche chambers, then results in copious quantities of UV photons emitted during charge multiplication [13]. This light can then be used to encode each event. In such a chamber, a 50 keV incident x-ray photon produces 2.10^7 UV photons (peaked at 280 nm). This yield is 4 orders of magnitude greater than a NaI crystal and 3 orders of magnitude greater than the yield from a gas scintillation proportional counter (in which no charge multiplication takes place). It ensures excellent spatial resolution at low energies with a conventional Anger camera arrangement, and is also sufficient to drive a focusing system with an intensified CCD camera. Both approaches are being investigated.

A Hybrid Detector: Phoswich detectors are used extensively in hard x-ray/ gamma ray astronomy, but suffer from poor performance at low energies due to the small number of visible photons produced by the NaI crystal. The hybrid instrument [14, optically couples a 40 cm x 40 cm phoswich, currently

under development at HCO/CfA [15], to the avalanche chamber described above, and utilizes a common photomultiplier array to read out the light from both sections. The avalanche chamber provides low energy response, while at high energies the gas becomes transparent and the incident photons interact directly with the scintillator.

The addition of the gas detector offers significant improvements over the bare phoswich - approximately a factor of two in energy resolution and improved spatial resolution. For single events, around 1mm is achievable at 25 keV, compared with 16 mm for the bare crystal. For fluorescent pairs (section 2.1) simulations show that the very high light yield from the chamber still permits the true position of each event to be deconvolved from the overlapping light distributions despite the coarse 7 x 7 photomultiplier array [13].

With phoswich type rejection in the scintillator, escape-gating rejection in the gas detector together with risetime discrimination and the possibility of mutual rejection between the two sections, the hybrid offers broad-band high-sensitivity coverage which greatly improves the standard phoswich for little added complexity. A 1/2 scale prototype is under construction to resolve remaining design questions [16].

An Imaging Polarimeter: The copious light emission from the optical avalanche chamber permits a CCD based optics system to be utilized for imaging the photoelectron tracks of x-ray interactions. Fig. 2a shows a typical arrangement where two stages of charge amplification are used to enhance light yield and to facilitate gating. At low energies, where diffusion dominates, the spatial resolution is limited to of order 1 mm. At higher energies, where the track is more extended, software can be developed to follow the convoluted path of the electron back to its origin and the resolution becomes essentially independent of energy. Fig. 2b shows a typical photoelectron track in 2 atm of argon. Measurements of the ionization density in the track can facilitate charged particle rejection. In addition, measuring the photoelectron ejection angle leads to polarization sensitivity as the electron is emitted preferentially in one direction for polarized x-rays. A modulation factor of 30% has been measured at 60 keV in a small prototype chamber. A (balloon-borne) flight instrument is currently being developed for the 35-70 keV range [17].

3.2 Medium Energy Regime (100 $keV - MeV$)

3.2.1 High-Pressure Proportional Counters

Proportional counters can be successfully operated at pressures much higher than 5 atm., although the operating voltage rises significantly and the energy resolution degrades. Sakurai et al. [18] and Sood et al. [19] have taken data in xenon up to 10 atm. and 17 atm. respectively, and each demonstrate the same trends although they interpret the resolution degradation

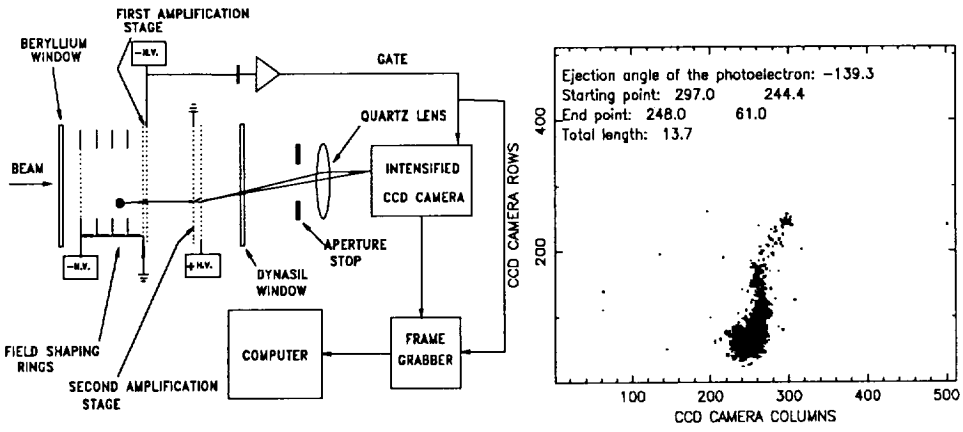

Fig. 2. a and b : Schematic of a CCD based x-ray imaging chamber and a 54 keV photoelectron track imaged in 2 atm of Argon + Trimethylamine.

in different ways. Whatever the exact mechanism, it seems that the reduced multiplication field at higher pressures plays a key role in this reduction and that , for operating pressures above 20 atm, the resolution of a practical proportional counter would probably be comparable to that of the solid scintillator. Despite this there may still be advantages with the high pressure proportional counter over the standard NaI scintillator [19].

3.2.2 High-Pressure Ionization Chambers

As outlined in section 2.3, the energy resolution of a proportional counter is severely degraded by the charge multiplication process, particularly at high pressures. If used in the ionization mode, though, this resolution can theoretically approach the Fano limit involving only the statistics of the initial ionization process. In this case a resolution of less than 0.5% would be achieved at 1 MeV in xenon, which is within a factor of three of the theoretical resolution of germanium solid state detectors.

Several types of high-pressure ionization chambers have been investigated including parallel plate and cylindrical detectors with and without shielding meshes [20,21]. In practice the resolution is found to be limited by preamplifier noise, acoustical noise and physical processes in the gas. Fig. 3 shows the energy resolution at 570 keV as a function of xenon density [22]. Below 0.5 gm/cm^3 the energy resolution is approximately constant and approaches the Fano limit. Above this density a sharp degradation of energy resolution takes place which, it is suggested, is caused by increasingly large fluctuations of charge recombination in the high-electron-density delta rays. It may be that this effect can be reduced, as with liquid xenon detectors, by doping with a photosensitive vapor having an ionization potential below the energy

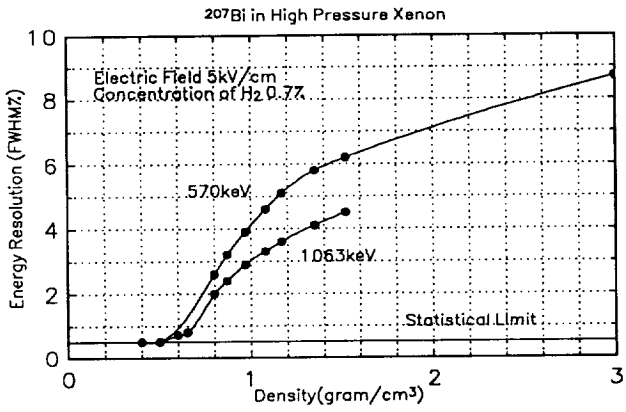

Fig. 3. Energy resolution as a function of xenon fill-gas density in a gridded ionization chamber

of the UV (xenon) photons emitted in the recombination process. This has the effect of decreasing the charge density in the delta rays and reducing the recombination effect [23]. Another explanation may be the formation of molecular clusters in the xenon which can trap electrons. The onset of this clustering is around 0.5 gm/cm^3 at room temperature [24]. If this mechanism is correct, warming the high pressure gas at densities above 0.5 gm/cm^2 could improve the resolution to that seen at lower densities.

An imaging high-pressure detector can be envisioned from an array of vertically cylindrical ionization chambers, with spatial resolution set by each tube diameter. It may further be possible to segment the collection anode, to derive an azimuthal co-ordinate within each detector and to use signal risetime to get a radial co-ordinate. The precision of such techniques, and the low-energy performance of such detectors is critically dependent upon the preamplifier noise. It may be possible to achieve around 50 electrons rms with modern (optical feedback, or no feedback) amplifiers resulting in an energy resolution of a few percent at 100 keV.

3.3 High-Energy Regime ($MeV - GeV$)

3.3.1 Drift Chambers and RICH detectors

When used in conjunction with a suitable converter, or sometimes without if the gas pressure is high enough, gas detectors can be used to image the charged particle tracks resulting from pair production. A three-dimensional reconstruction of these tracks permits the initial photon direction to be recovered. The proposed AGATE detector, successor to EGRET, utilizes stacks of large area (1/2 m x 1/2 m), thin (1 cm deep) drift chambers to reconstruct slices of the tracks with high precision over a proposed energy range from 20 MeV to 100 GeV [25].

The positron/electron tracks can also be reconstructed by making use of the rings of Cherenkov light emitted by the charged particles as they traverse gaseous radiators – this is the basis of the Ring Imaging Cherenkov (RICH) detector. The Cherenkov light must be focused onto a suitable detector such as a UV-windowed imaging gas detector containing a photosensitive vapor such as TMAE. Running at high gain, these detectors are sensitive to single UV photons in the Cherenkov light ring with a resolution of around 2-3 mm [26]. An alternative to this approach is to use a solid radiator as the primary converter as was proposed in [27]. Here a TMAE gas-filled UV photon detector was also used but in a very-high-gain (10^6) multistep mode to produce large quantities of visible photons which are in turn imaged by an intensified CCD camera. With this arrangement a spatial resolution of 220 μm was achieved for single UV photon detection. An ultimate angular resolution of less than 1 degree was claimed for GeV energy photons.

References

1. Pfeffermann, E. *et al.*: 1986, *SPIE* **733**, 519
2. Brinkman, A.C. *et al.*: 1983, *Non-Thermal Processes and Very High Temperature Phenomena in X-Ray Astronomy*, Publisher:Rome, 263
3. Waldron, L. *et al.*: 1993, *SPIE* **1948**, 98
4. Ubertini, P. *et al.*: 1994, this volume
5. Bateman, J. E: 1984, *Nucl. Instr. and Meth. in Phys. Res.* **221**, 131
6. Dietz, K.L. *et al.*: 1993, *Space Programs and Technologies AIAA conference* **AIAA 93**, 4254
7. Ramsey, B.D. *et al.*: 1989, *Nucl. Instr. and Meth. in Phys. Res.* **A278**, 576
8. Alkhazov, G.D.: 1970, *Nucl. Instr. and Meth.* **89**, 155-165
9. Oed, A.: 1988, *Nucl. Instr. and Meth. in Phys. Res.* **A263**, 351-359
10. Ramsey, B.D.: 1992, *SPIE* **1743**, 96
11. Budtz-Jorgensen, C. *et al.*: 1992, *SPIE* **1743**, 162
12. Ramsey, B.D. *et al.*: 1994, *SPIE* **2280**, 576
13. Ramsey, B.D. *et al.*: 1993, *SPIE* **2006**, 90
14. Grindlay, J.E. and Manandhar, R.P.: 1989, *SPIE* **1159**, 306
15. Manandhar, R.P. *et al.*: 1993, *SPIE* **2006**, 200
16. Pimperl, M.M. *et al.*: 1994, *SPIE* **2280**, 119
17. Austin, R.A. and Ramsey, B.D.: 1993, *Optical Engineering* **32(8)**, 1990
18. Sakurai, H. *et al.*: 1991, *Nucl. Instr. and Meth. in Phys. Res.* **A307**, 504
19. Sood, R.K. *et al.*: 1994, *Nucl. Instr. and Meth. in Phys. Res.* **A344**, 384
20. Dimitrenko *et al.*: 1992, *SPIE* **1734**, 295
21. Levin, C. *et al.*: 1993, *Nucl. Instr. and Meth. in Phys. Res.* **A332**, 206
22. Bolotnikov, A.E. *et al.*: 1986, *Translation in Instrum. Exp. Tech.* **29**, 802
23. Masuda, K. *et al.*: 1994, SPIE 2305
24. Bolotnikov, A.: 1994, private communication
25. Mukherjee, R. *et al.*: 1994, SPIE 2305
26. Swordy, S.: 1994, *Nucl. Instr. and Meth. in Phys. Res.* **A343**, 52
27. Charpak, G.: 1994, *Nucl. Instr. and Meth. in Phys. Res.* **A343**, 300